



## **EXPERIMENTAL TEST ON A FULL SCALE REPAIRED R.C. STRUCTURAL WALL**

**Paolo RIVA<sup>1</sup>, Alberto MEDA<sup>2</sup> and Ezio GIURIANI<sup>3</sup>**

### **SUMMARY**

In the present research, the structural behaviour of a full scale structural wall, representative of a four storey building, with one underground storey and a box foundation system, repaired after heavy damage simulating a design earthquake, is experimentally studied under transverse cyclic loads.

The original wall, designed according to Eurocode 8 [1-3] assuming a peak ground acceleration  $a_g = 0.20$  g, considering a structural coefficient  $q = 3$ , was tested under cyclic loading up to failure, which was due to sliding shear [4, 5]. After the test, the wall was repaired, substituting the yielded rebars with new ones, and increasing shear reinforcement in the critical section. The repaired wall was tested with the same loading history of the previous test.

The response of the repaired wall was satisfactory only up to yielding, whereas only a few cycles at the yield displacement could be performed prior to collapse. Although the results were not as good as hoped, useful indications could nonetheless be obtained on the feasibility and necessary improvements of the adopted solution.

### **INTRODUCTION**

Seismic resistance of r.c. structures is often assigned to structural walls, with the columns resisting mainly vertical actions. Compared to frame resistant systems, such structures are stiffer and have the advantage of limiting damage to the external and internal partitions and infill walls, while the drawbacks are related to lower ductility and larger seismic forces.

Extensive experimental results concerning the behaviour of walls of different slenderness ratio subjected to various loading conditions are available in the literature (e.g. [6-11]). These tests are generally limited to small scale specimens, typically from 1:2 to 1:3 scale. The results have shown that the inelastic response of slender walls, characterized by height-over-width ratios larger or equal to 2, is controlled by flexural deformations in a plastic hinge at the base of the wall.

---

<sup>1</sup> Associate Professor, Dept. of Civ. Engrg., University of Brescia, Italy – E-Mail: riva@ing.unibs.it;

<sup>2</sup> Assistant Professor, Dept. Eng. Techn. and Des., Un. of Bergamo, Italy – E-Mail: meda@ing.unibs.it;

<sup>3</sup> Professor, Dept. of Civ. Engrg., University of Brescia, Italy – E-Mail: giuriani@ing.unibs.it;

The behaviour of a full scale shear wall of a four storey building, with one underground storey and a box foundation system was tested by the Authors [4, 5]. The results demonstrated that the service behaviour was mostly linear elastic, with reduced damage and small dissipated energy, while the behaviour after yielding showed a progressive damage of the wall with increasing imposed displacement cycle amplitude. The damage was mainly localised at the critical section, where cracking progressively developed into large, wide open cracks, and concrete crushing was observed. A considerable ductility, ensuring the required design value, was obtained, although the collapse was governed by sliding shear, with formation of a single large crack near the base section.

Following the test, the possibility of repairing the tested wall was investigated. Current repair techniques for reinforced concrete buildings following earthquake damage are extensively reviewed in [12, 13]. The suggested solutions mainly concern beams, columns, beam-column joints. As for structural walls, repair solutions with either added reinforcement or FRP confinement have been adopted for weakly damaged walls. Little is available concerning the repair of heavily damaged structural walls, like the one tested by the Authors.

Accordingly, a reconstruction of the wall at the ground floor level, next to the critical section, was attempted, with the objective of ensuring the same flexural strength and ductility of the undamaged wall, as well as to provide an increased sliding shear strength, with the aim of avoiding the previously observed early shear failure.

Although the experimental setup would have allowed the reconstruction of a large section of the wall, a repair strategy was developed with the aim of reproducing a more realistic situation, where the presence of floor slabs would have suggested to limit the works to the clear span between the ground and the first floor.

The repaired wall was finally tested following a loading history similar to the one adopted for the original wall. The response of the repaired wall was satisfactory only up to yielding, whereas only a few cycles at the yield displacement could be performed prior to collapse. Although the results were not as good as hoped, useful indications could nonetheless be obtained on the feasibility and necessary improvements of the adopted solution.

## **TEST SET UP**

The structural wall was designed according to EC8 [1-3], assuming a structural coefficient  $q = 3$  and a peak ground acceleration  $PGA = 0.20 g$ , typical for medium seismicity zones. A higher ground acceleration could not be adopted, due to limitations in the testing loading frame available. Verification of sectional strength was carried out according to Eurocode 8 and Eurocode 2 [1-3, 14].

Figure 1 illustrates the wall dimensions and steel reinforcement detailing. The wall dimensions were: section 2800x300 mm outside of the supports, 2800x400 mm between the supports, length outside the supports 12 m, and 15.5 m total length. At the ground and basement levels, two ribs were inserted to simulate the floor diaphragms, typical of a box foundation. A detailed description of the wall design hypotheses may be found in [4, 5].

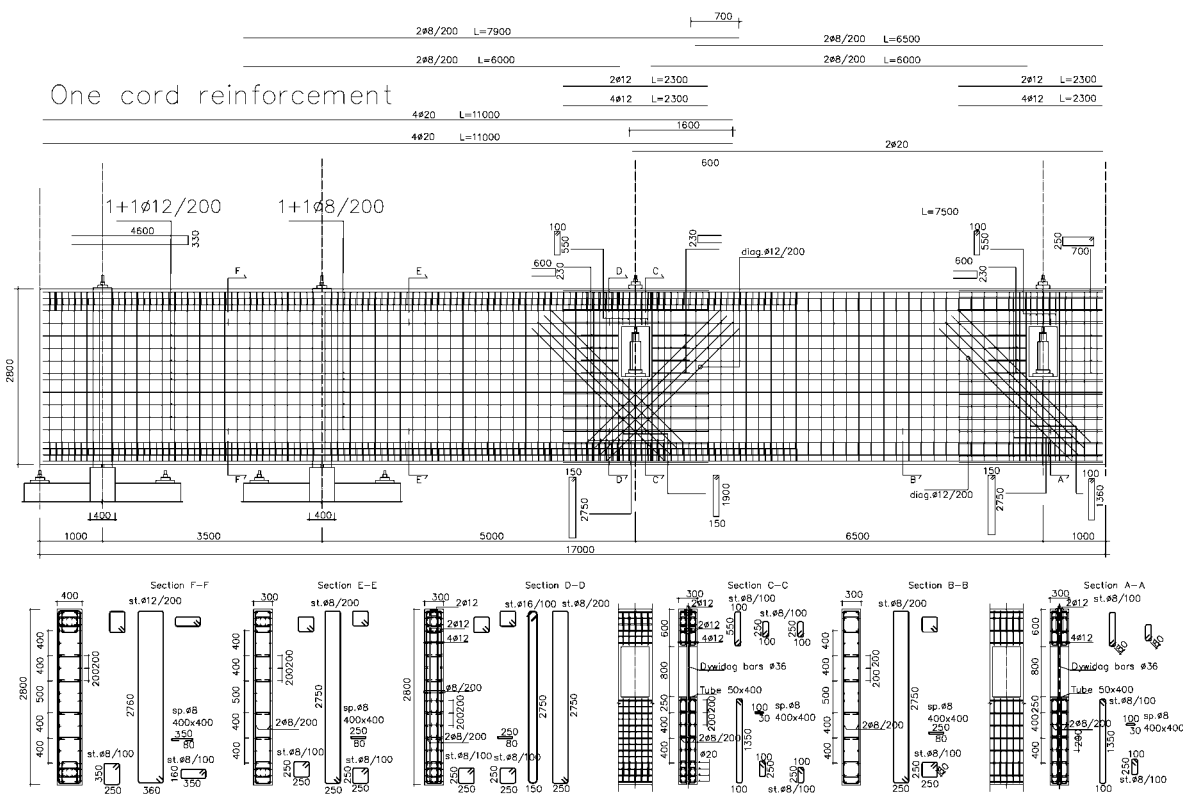


**Figure 1 – Original wall layout and reinforcement.**

Being the reaction structure available a prestressed concrete underground caisson, which allows testing structures of span up to 40m, the wall had to be placed horizontally, keeping the axis of maximum inertia vertical, as shown in Figure 2. The wall was placed on two r.c. supports (a in Figure 2), aligned with the ribs simulating the ground and basement floor diaphragms (b in Figure 2), and fixed to the caisson by adopting post tensioned 0.6” strands and high strength  $\phi 32$  bars (c in Figure 2). Strands and bars post tension was such that no decompression of the support would occur during testing.

Two steel frames (d in Figure 2) were placed near the loading positions in order to avoid lateral instability. The safety of the system was improved by inserting a supplementary frame between the two supports (e in Figure 2), which would intervene whenever a lack in post-tension would induce a support decompression.

The loads were applied at two points by means of hydraulic jacks. The position of the jacks was defined to obtain the same bending moment and shear force around the critical section as the one resulting from the analysis of the four storey building (Figure 3). Moreover, the load position was such that the same force could be applied, greatly simplifying load control. Further details may be found in [4, 5].

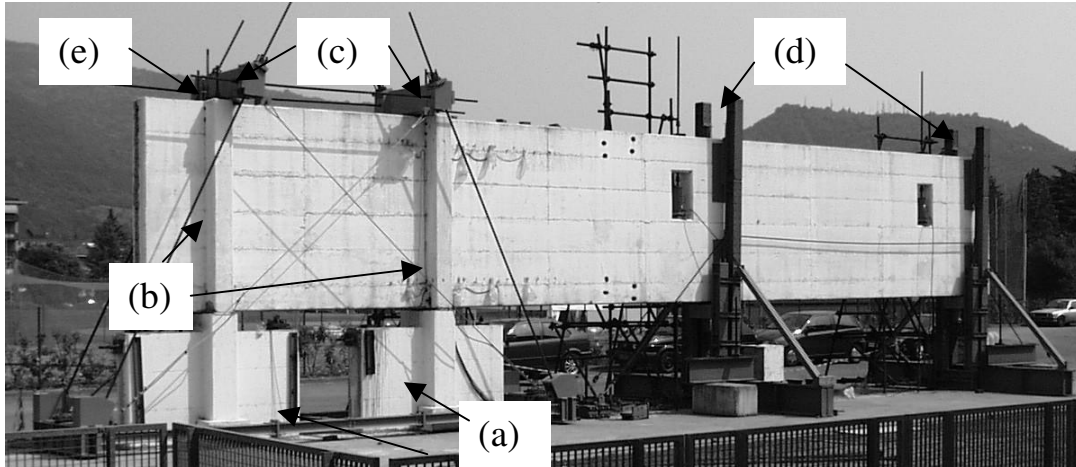


**Figure 2 – Test set-up: wall supports (a); ribs simulating the ground and basement floor diaphragms (b); post tensioned strands and bars (c); steel frame to avoid lateral instability (d); additional frames for improving safety in the test set-up (e).**

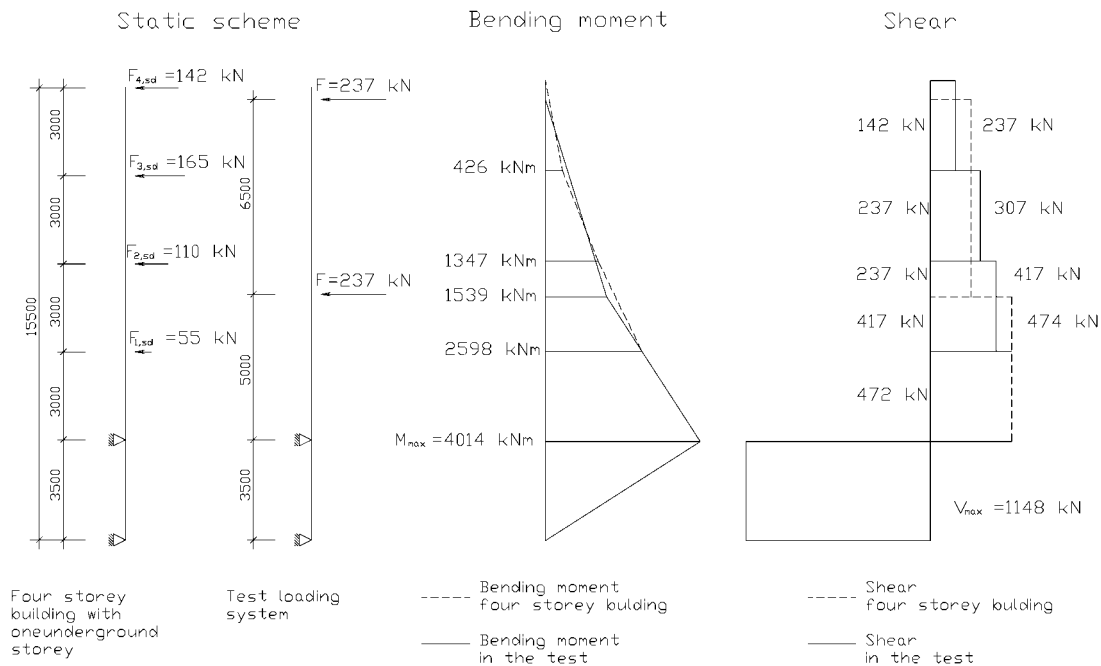


**Figure 3 - Action diagram: comparison between true scheme and the two jacks scheme.**

In order to apply cyclic reverse loads, four single stroke jacks were adopted, two acting upward (a in Figure 4) and two downward (b in Figure 4). The jacks acting upward were placed between the wall and the loading bench, while those acting downward were placed in two windows opened in the wall and connected to the caisson with two high strength  $\phi 32$  bars. The position of the opening was such that the jack would act along the wall neutral axis, thus limiting their horizontal displacement.

The applied load was measured by means of a full bridge resistive pressure transducer placed on the pump manifold. The displacement were measured using 17 potentiometric transducers as shown in Figure 4: two wire transducers (16, 17) measured the vertical displacement of the wall; 11 linear transducers (1-8, 14, 15) measured the displacements in the upper and lower chords close to the critical section; two linear

transducers (11, 12) were used for monitoring the deformation of the panel between the supports; two linear transducers (9, 10) measured the displacement between the wall and the caisson at the supports in order to monitor any potential support decompression. All the signals were conditioned by adopting a data acquisition system (Mod. UPM 100 by HBM) and recorded on a PC.

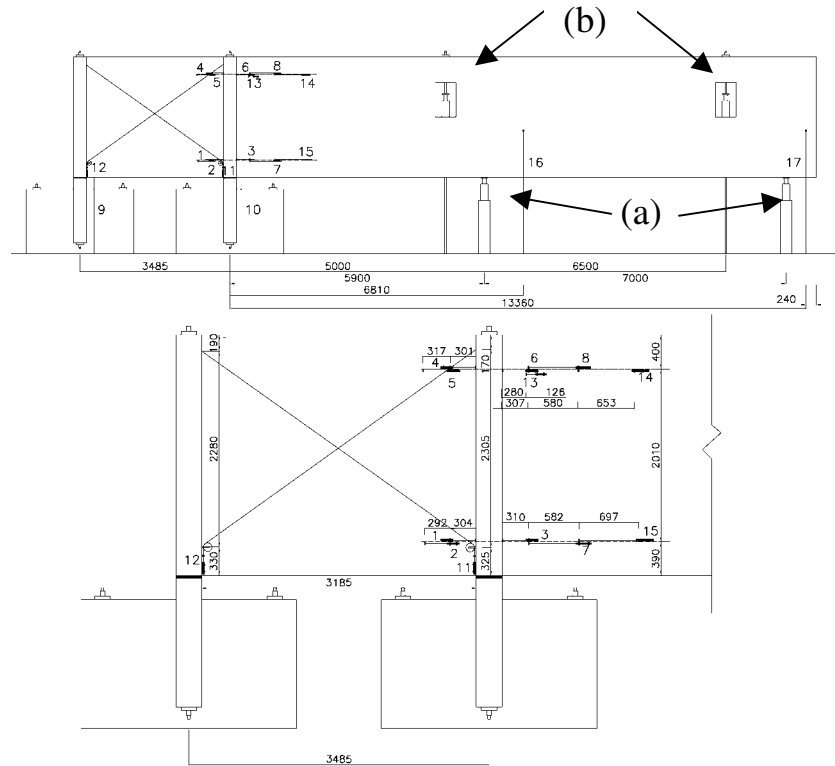


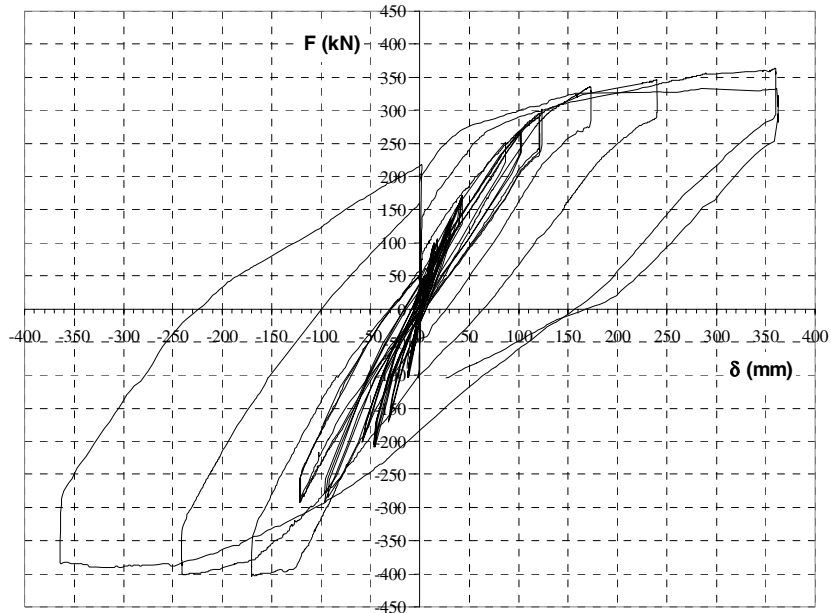
**Figure 4 – Jack positions (upward jacks (a) and downward jacks (b)), and measurement devices.**

### COLLAPSE OF THE ORIGINAL WALL

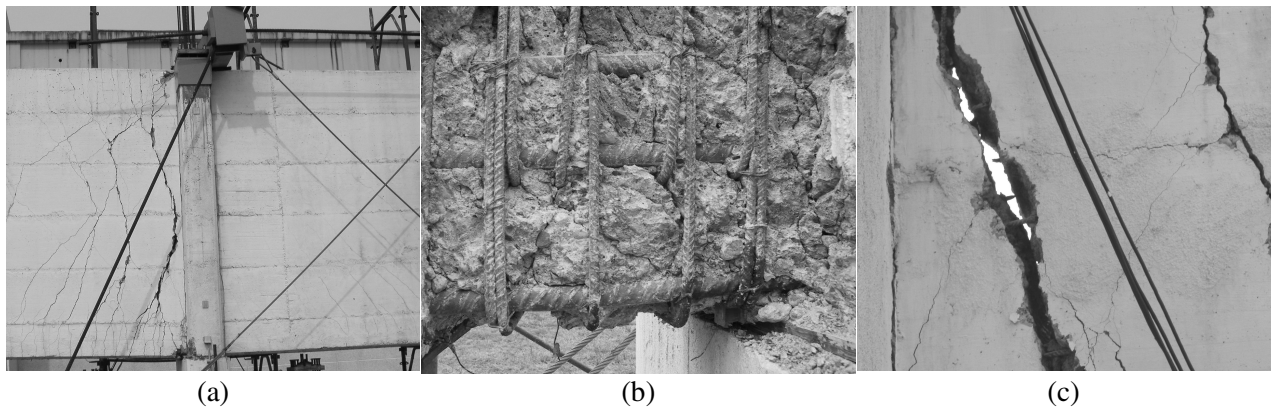
The description and discussion of the test on the original wall may be found in [4, 5]. Only the main results and the collapse mechanism will be recalled herein.

Figure 5 shows the force-versus-top displacement response of the wall up to collapse. The wall yielded at a displacement amplitude approximately equal to  $\delta_y = 120$  mm. Collapse occurred during the second cycle at  $3\delta_y = 360$  mm due to sliding shear failure. A stable structural response was observed up to collapse. In fact, no significant strength and/or stiffness degradation was observed during cycles following yield.

Figure 6a illustrates the critical region at collapse. A wide opened, arched crack is observed next to the support section. This crack developed after yield, when several smaller flexural cracks, starting from the outer chords, merged into a single crack. The main crack exhibited a maximum opening of approximately 50 mm towards the wall mid-depth and 10 mm at the chords. In the chords, concrete spalling, due both to compression forces and rebar bending, was observed (Figure 6b). The large crack opening in the middle part of the wall led to a marked strain localization in the longitudinal shear reinforcement, resulting in its tensile failure with necking (Figure 6c).



**Figure 5 - Force  $F$  versus end displacement  $\delta_y$  for the cycles after  $\delta_y$ .**



**Figure 6 – Detail of collapse mechanism.**

Concerning shear strength, the wide crack opening observed is not compatible with any aggregate interlock effect. Furthermore, the subsequent failure of the longitudinal panel reinforcement lead to a considerable reduction in the shear strength for dowel action. As a consequence, a shear failure occurred during the unloading phase, when the beneficial effect of compression in the upper chord, which enables the shear strength contribution due to friction, ceased to exist. Figure 6b shows that the main rebars are bent due to dowel action and consequent vertical wall displacement.

Regardless of the early shear failure, it is important to note that the ultimate displacement is nonetheless very large, being  $\delta_u = 360 \text{ mm} \approx 1/35$ ,  $l = 12.50 \text{ m}$  being the wall height. Furthermore, the maximum obtained displacement is sufficient to ensure the design required ductility, which, based on a theoretical yield displacement  $\delta_{yt} = 90 \text{ mm}$  and a structural coefficient  $q = 3$ , would have required an ultimate displacement at least equal to  $3\delta_{yt} = 270 \text{ mm}$ .

Finally, the stability of the wall response up to collapse leads to the conclusion that a considerable ductility margin was still available with respect to bending failure and that the shear reinforcement provided at the critical section was insufficient to avoid an early sliding shear failure.

## **WALL REPAIR**

In order to investigate the feasibility of a repair of a wall following heavy earthquake damages, a reconstruction of the wall at the ground floor level, next to the critical section, was attempted.

The repair strategy had the objective of ensuring the same flexural strength and ductility of the undamaged wall, as well as to provide an increased sliding shear strength, with the aim of avoiding the previously observed early shear failure.

Although the experimental setup would have allowed the reconstruction of a large section of the wall, a repair strategy was developed with the aim of reproducing a more realistic situation, where the presence of floor slabs would have suggested to limit the works to the clear span between the ground and the first floor.

The following operations were therefore devised:

1. concrete demolition by jack-hammer for a height slightly smaller than one interstorey (2.50 m);
2. measure of the residual (plastic) deformation of the main longitudinal rebars in the chords;
3. substitution of all longitudinal reinforcement showing plastic deformations higher than 1%, which is approximately equal to the strain hardening limit for current European steel;
4. substitution of the longitudinal and transverse shear reinforcement, which failed during the previous test;
5. introduction of supplementary longitudinal web reinforcement, with the aim of increasing the sliding shear strength;
6. cast in-place of new concrete with the same section geometry of the original wall.

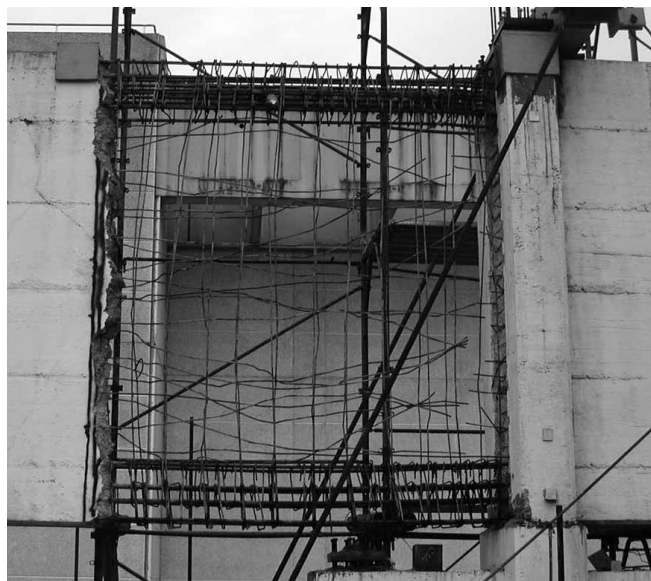


**Figure 7 – Critical region after concrete demolition.**

Figure 7 shows the critical section after the demolition. As expected, all of the longitudinal web reinforcement was cut next to the base section, where the main crack had occurred (Figure 6b). A maximum residual deformation approximately equal to 5%, evaluated by measuring with a caliber the rib spacing in the deformed bars, was measured in the outermost rebars next to the critical section. Non negligible residual deformations were measured in all the bars in the chords and in most of the demolished region, whereas no residual deformations were observed towards its end.

Given the above, all of the bars in the chords had to be replaced. Since lap-splicing could not be adopted, due to an insufficient development length, mechanical couplers (Ancon<sup>®</sup> MBT, Figure 8) were used to link the new bars to the existing ones.

In order to avoid cracking due to bearing stress acting on the mechanical couplers of the main rebars in the critical section, the base section was transversally confined and widened for all of the coupling length (0.50 m), adopting the same width of the diaphragm (Figure 8). In order to transmit, by dowel action, the total base shear between the newly cast and the old concrete 16  $\phi 26@200\text{mm}$ , 400mm long, grouted studs were inserted in the existing diaphragm (Figure 8).

Concerning web reinforcement, the original longitudinal and transverse  $\phi 8@200\text{mm}$  bars were replaced with new rebars, grouted for a depth of 100 mm into the ground floor diaphragm, and spliced to the original web reinforcement at the other end. In order to improve sliding shear strength, 28 $\phi 12@135\text{mm}$  longitudinal bars and  $\phi 8@200\text{mm}$  stirrups were added in the middle portion of the wall next to the base section. In the attempt to control the arched crack which led to the original wall collapse (Figure 6a), and to force the formation of a diffused truss mechanism, the longitudinal additional reinforcement was placed as shown in Figure 8.

For further safety of the testing setup, eight external, post-tensioned, unbonded,  $\phi 32$  Dywidag<sup>®</sup> bars were added between the two diaphragms, along the part of the wall simulating the underground floor of the box foundation (Figure 8).

A concrete class C30/37 was used for the repair. The average cube strength of the new concrete was equal to  $f_{c,cube} = 41.8$  MPa, as opposed to the original one, equal to  $f_{c,cube} = 40.7$  MPa.

The bending and shear strength at the critical section of the repaired and original wall are compared in Table 1.

**Table 1 – Bending and shear strengths at the base section of the original and repaired wall.**

Original Wall		Repaired Wall	
$M_{Rd} = 4015$ kNm	$V_{Rd,truss} = 790$ kN	$M_{Rd} = 6014$ kNm	$V_{Rd,truss} = 865$ kN
	$V_{Rd,sliding} = 715$ kN		$V_{Rd,sliding} = 1191$ kN
$M_{y,exp} = 5300$ kNm	$V_{y,exp} = 615$ kN	$M_{y,exp} = 5155$ kNm	$V_{y,exp} = 652$ kN
$M_n = 5910$ kNm	$V_n = 1165$ kN	$M_n = 6420$ kNm	$V_n = 1225$ kN

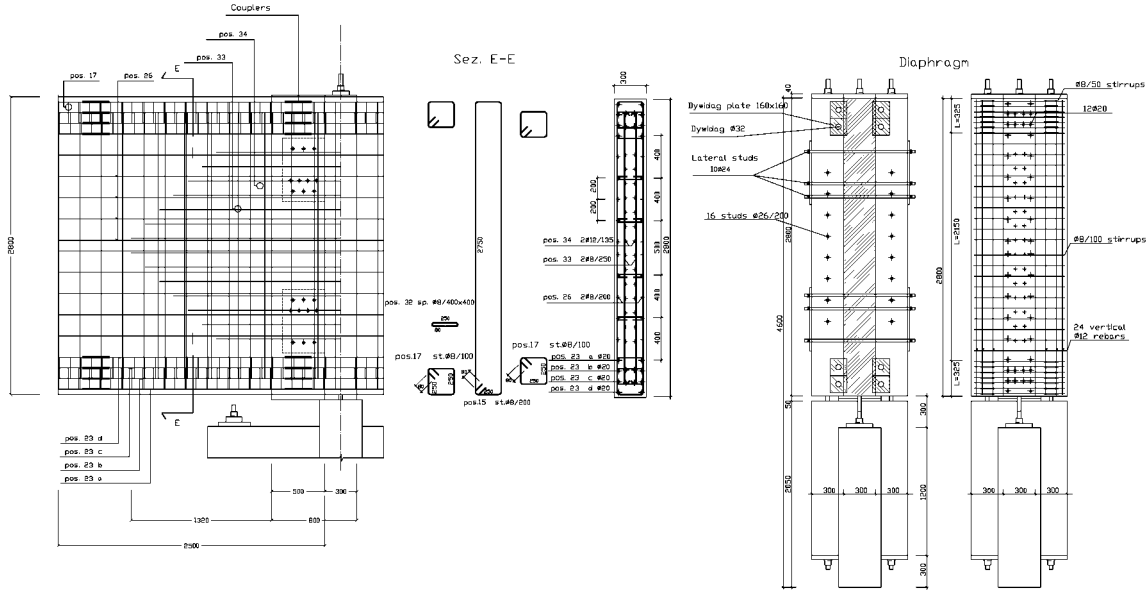


**Figure 8 – Reinforcement detailing for the repaired wall.**



**Figure 9 – Repaired critical region before concrete casting.**

## EXPERIMENTAL TEST ON THE REPAIRED WALL

### Behaviour up to first yield

The behaviour of the repaired wall up to the theoretical first yield load ( $F_{yt}$ ), defined as the load for which the theoretical yield moment ( $M_{yt}$ ) at the base section is reached, was initially investigated. The yield bending moment, defined by imposing that the strain in the external reinforcement is equal to  $\epsilon_{sy} = f_{sy}/E_s = 540/206\,000 \approx 0.26\%$ , and yield load were equal to  $M_{yt} = 5160$  kNm, and  $F_{yt} = 277$  kN, respectively, while the corresponding theoretical end displacement is equal to  $\delta_{yt} \approx 100$  mm.

Figure 10 illustrates a comparison of the applied force-vs-end displacement response of the repaired and original walls. The repaired wall has a stiffness comparable to the original one, while a more pronounced hysteretic behaviour is evident.

The crack pattern at the yield load for the two situations is shown in Figure 11. This Figure demonstrates that a more diffused crack pattern developed in the repaired wall, while in the original one the cracks tend to merge towards the base section, forming the arched crack which eventually led to collapse. Furthermore, the devised diffused truss mechanism was observed in the repaired wall.

No relevant differences were found in the zone between the supports for the two walls. A diffused crack pattern was detected in both cases, with a crack inclination of about  $45^\circ$ , typical of panels loaded by pure shear, and a reduced crack opening (lower than 0.1 mm).

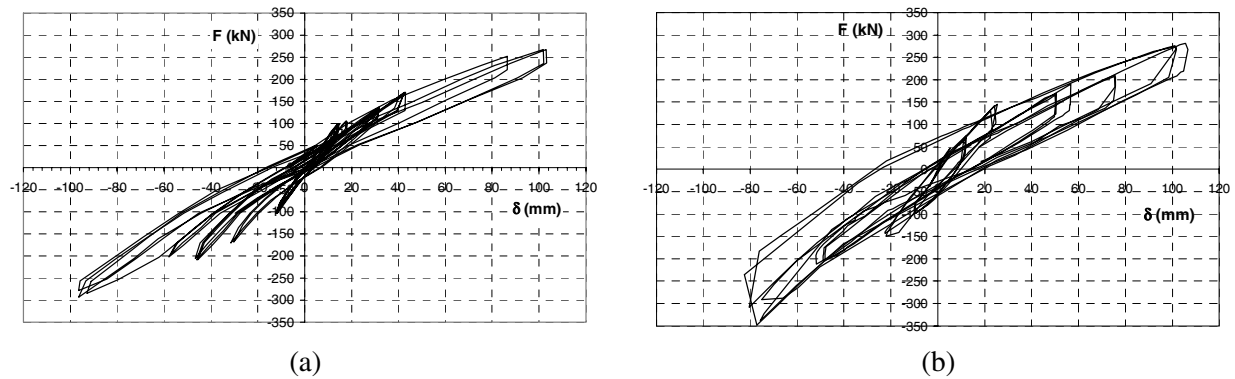


**Figure 10 – Comparison of the original (a) and repaired wall (b) response up to yielding.**

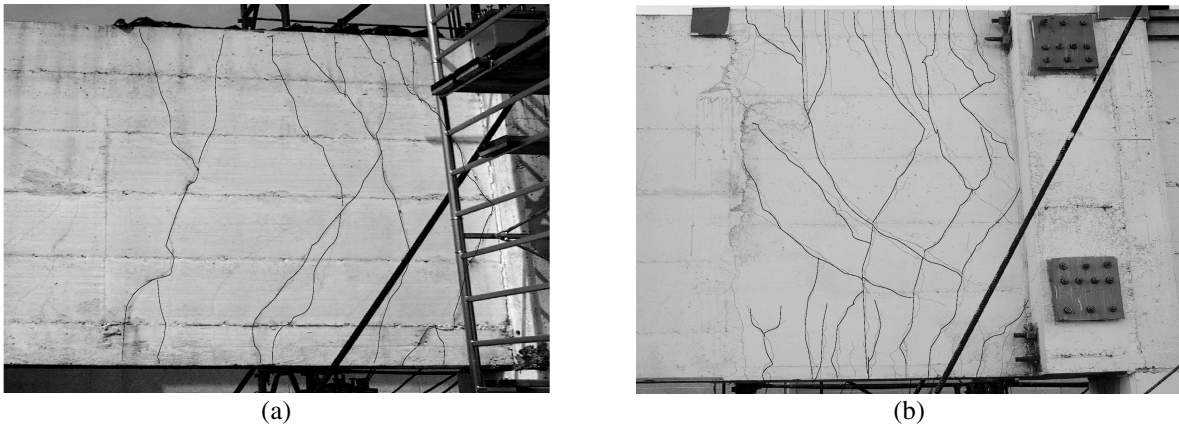


**Figure 11 – Comparison of the original (a) and repaired wall (b) crack pattern at yield.**

### Behaviour up to collapse

Figure 12 illustrates the loading history adopted during the test. In order to find the structural yield displacement, the load was initially increased until the intersection between two lines tangent to the load-displacement curve in the II stage (after cracking) and in the III stage (after yielding) could be determined in both loading directions. The yield displacement was found to be approximately equal to  $\delta_y \approx 135$  mm.

During the first cycle, while determining  $\delta_y$ , a large shear crack appeared close to the end of the repaired wall section (Figure 13a). After load reversal, a similar crack developed starting from the lower chord and merged to the previous one (Figure 13b). During the second cycle at  $\delta_y$ , severe concrete spalling was

observed in the upper chord, close to the end of the rebar couplers location (Figure 13c). After completion of this cycle, the test was interrupted, and the spalled concrete was removed.

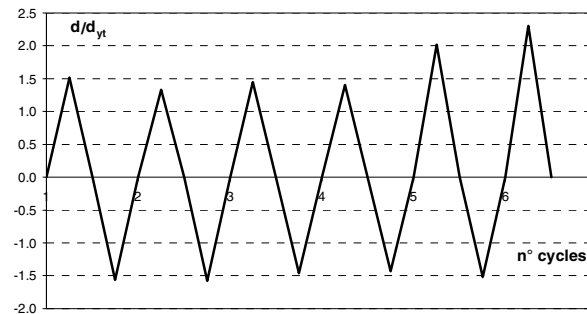


**Figure 12 – Loading history from yielding to failure.**

Figure 13d shows that the outer longitudinal bars buckled next to the couplers. This phenomenon has been interpreted as a consequence of the compression bearing stress on the couplers end sections close to the concrete cover, where concrete confinement is not effective. Hence, a strengthening of the damaged section was necessary. The same problem, although less evident, was observed also in the lower chord.

Accordingly, the buckled bars were straightened and the couplers were connected together with welded steel plates, in order to prevent any possible future buckling phenomenon (Figure 13e). The main crack was widened and filled with high strength concrete mortar. Finally, the damaged concrete in the chords was replaced with the same mortar.

To confine the chords, two steel caps were placed and prestressed across the section, by means of three threaded  $\phi 20$  bars. The section was further confined by means of two external unbonded, prestressed  $\phi 26$  Dywidag® bars, placed as shown in Figure 13f.

After this repair, the test continued with a third cycle at  $\delta_y$ . During this cycle, the repaired main crack reopened. At this point, the confinement was extended, doubling the steel caps and confining bars (Figure 13g).

After this last repair, a fourth cycle at  $\delta_y$  was successfully completed. During the following cycle at  $1.5\delta_y$  the wall finally collapsed, once again due to the opening of the same crack (Figure 13h), which lead to a very large strain localisation in the web reinforcement, which failed in tension, likewise what was observed during the third cycle at  $3\delta_y$  in the original wall (Figure 6). The experimental behaviour following the theoretical yield is presented in Figure 14 (load versus end displacement  $F-\delta$ ), where the results of the original and repaired walls are compared.

These Figures show that the structural yield point is almost the same for both walls. The response up to collapse of the repaired wall did not show any significant unstable behaviour and no significant pinching in the cycles appeared. In both cases, an anticipated collapse related to shear was observed, and the full bending ductility could not be developed. The collapse mechanisms for both the original and repaired walls are shown in Figure 15.

In any event, the repaired wall showed a good behaviour only up to the structural yield. After this point, the presence of the mechanical couplers caused an excessive local damage in the outer chords due to compression bearing stress. Even after having heavily confined the section next to the couplers, shear collapse could not be prevented. In fact, once the main crack opened in bending at the chords, it further

developed due to a lack of web reinforcement. Under this respect, it is important to note that the shear crack developed outside of the theoretical critical section, which had a heavy web reinforcement against sliding shear.

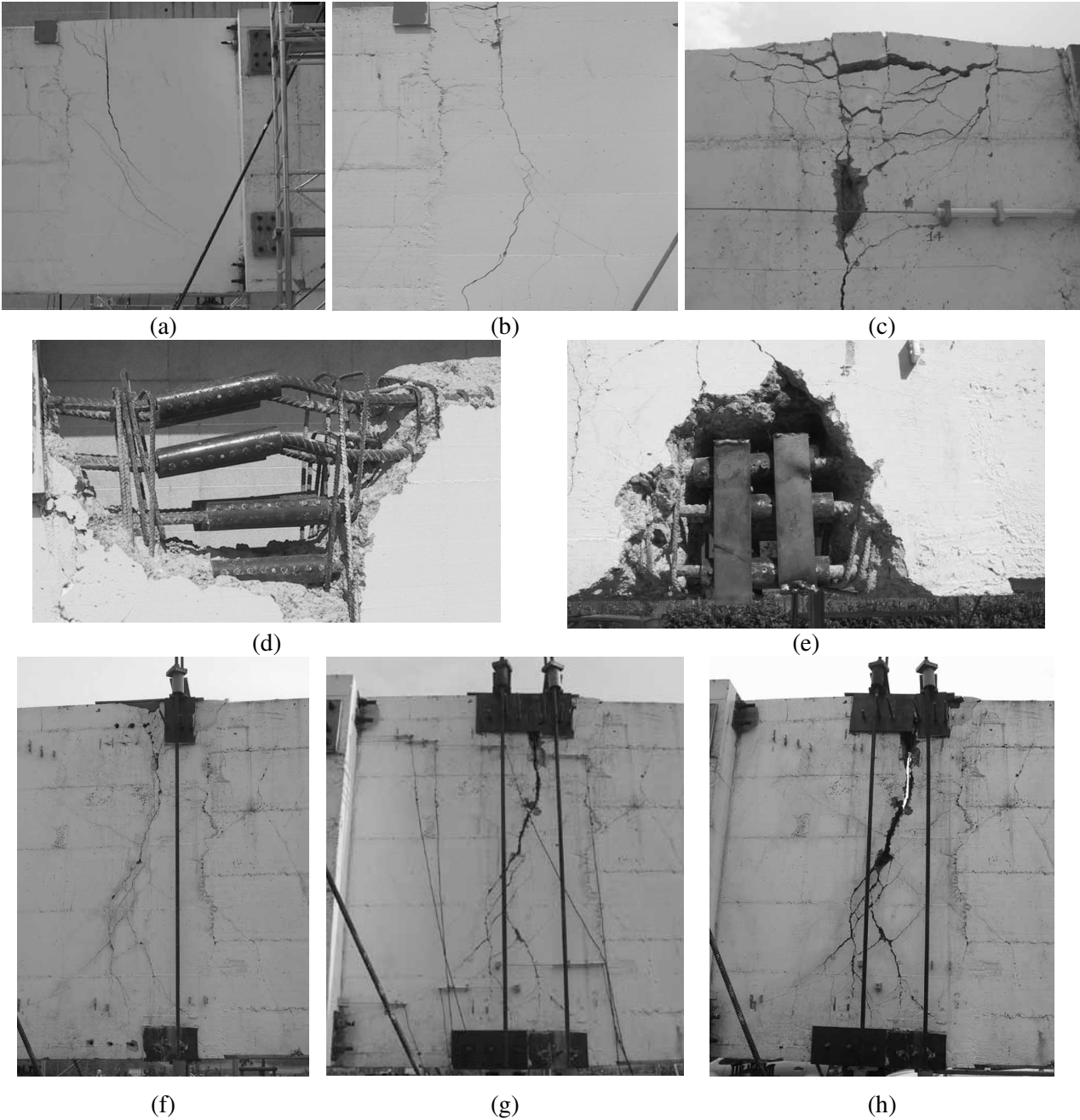


**Figure 13 – Development of damage up to failure of the repaired wall.**

It is furthermore observed that, while bending moment linearly decreases along the wall, shear action is constant next to the wall support (Figure 2). Hence, providing sliding shear overstrength only next to the base section, where the collapse of the original wall was observed, was not sufficient and somewhat detrimental. In fact, the added web reinforcement contributed to considerably increase the bending strength of the base section, moving the critical section closer to the end of the repaired part of the wall, where the mechanical couplers were present.

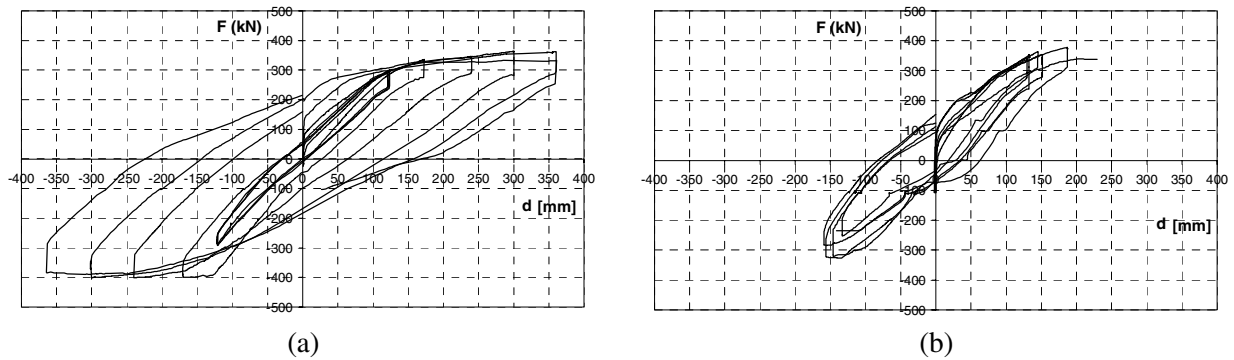


**Figure 14 – Comparison of the original (a) and repaired wall (b) response up to failure.**

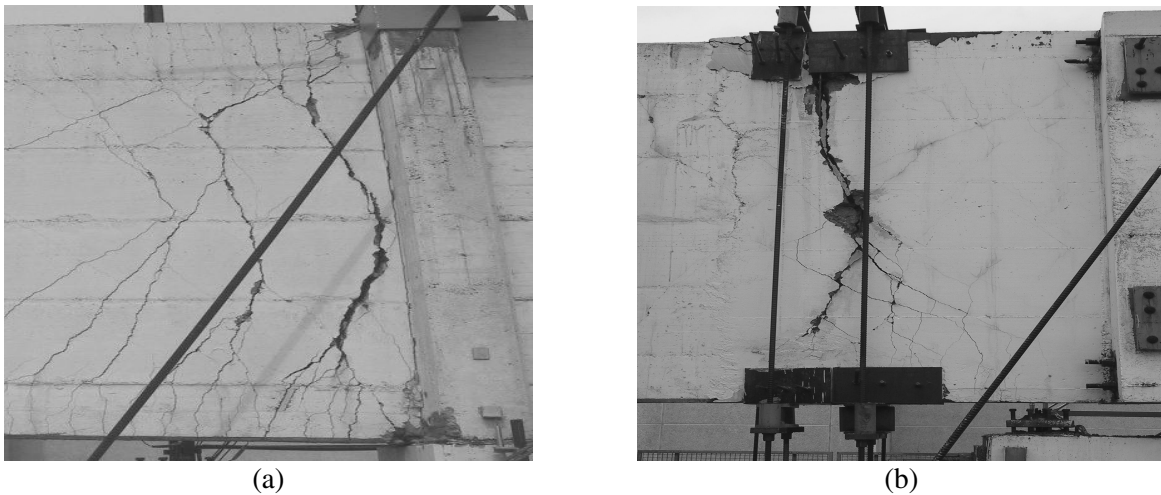


**Figure 15 – Comparison of the original (a) and repaired wall (b) failure mechanisms.**

The results also show that the longitudinal web reinforcement towards the end of the repair should have been better grouted into the old concrete, instead of being spliced to the original web reinforcement.

## CONCLUSIONS

The repair of a full size 12.5 m high structural wall, heavily damaged under transverse cyclic loads during a previous experimental test, has been presented. The repair consisted of replacing the reinforcement and casting new concrete in the lower part of the wall, for a length of 2.5 m from the base section, representing the area of the first interstorey. The repaired wall was then tested following a loading history similar to the one adopted for the original, unrepaired, wall.

The following is observed from the test results:

- Up to yield, the repaired wall has a stiffness comparable to the original one, while a more pronounced hysteretic behaviour was observed. The crack pattern at the yield load demonstrates that a more diffused crack pattern developed in the repaired wall, while in the original one the cracks tend to merge towards the base section, forming the arched crack which eventually led to collapse;
- During the second cycle at yield, severe concrete spalling was observed in the upper chord, close to the end of the rebar couplers location, due to compression bearing stress at the rebar coupler end location.

The same phenomenon was observed also in the lower chord during the following half cycle. Local confinement was therefore added in order to continue the test;

- Collapse was attained during the first cycle at  $1.5\delta_y$  due to shear, with a major crack developing from the end of the rebar couplers.

Based on the results, it is concluded that the repair was effective only up to yield. To improve the wall performance after yield, a few changes in the adopted repair solution are required. The main individuated deficiencies are: (i) use of flat-head rebar couplers in the chords induced heavy stress concentration due to bearing stress on the coupler end; (ii) extremely high confinement is needed in the coupling zone (e.g. stirrups, local increase of the wall thickness, FRP confinement, etc.); (iii) the extension of the supplementary shear reinforcement was not sufficient (e.g. supplementary shear reinforcement should be added to the whole repaired region to ensure adequate overstrength in a region of constant shear action).

### ACKNOWLEDGEMENTS

The research was co-financed by MIUR (Italian Ministry of University and Research) within the program COFIN-2002 "Retrofitting and experimental test of a full scale structural wall subjected to horizontal cyclic loads." Finally, the authors are grateful to Mr. Riccardo Giovanelli, Mr. Nicola Marcandelli, and Mr. Andrea Rossi who carried out the experimental test of the wall under their respective Master Thesis projects.

### REFERENCES

1. EUROCODE 8, "Design Provisions for Earthquake Resistance of Structures – Part 1-1: General rules, seismic actions and general requirements for structures", ENV 1998-1-1, 1994.
2. EUROCODE 8, "Design Provisions for Earthquake Resistance of Structures – Part 1-2: General rules – General rules for buildings", ENV 1998-1-2, 1994.
3. EUROCODE 8, "Design Provisions for Earthquake Resistance of Structures – Part 1-3: General rules – Specific rules for various materials and elements", ENV 1998-1-3, 1995.
4. Riva P, Meda A, Giuriani E. "Experimental test on a real size structural wall." *Engineering Structures* 2003; 25: 835-845.
5. Riva P, Meda A, Giuriani E. "Full scale test on a r.c. structural wall under cyclic transverse loads." *Proceedings of the fib 2003 Symposium, Concrete Structures in Seismic Regions, May 6-9, 2003, Athens.*
6. Paulay T, Priestley MJN. "Seismic Design of Reinforced Concrete and Masonry Buildings." J. Wiley & Sons, New York, 1992.
7. Paulay T. "Earthquake-Resisting Shearwalls - New Zealand Design Trends." *ACI Journal* 1980; 77(3): 144-152.
8. Bertero VV, Popov EP, Wang TY, Vallenias J. "Seismic Design Implications of Hysteretic Behavior of R.C. Structural Walls." *Proceedings of the 6th World Conference on Earthquake Engineering; New Delhi, 1977, vol.5, p. 159-165.*

9. Paulay T, Priestley MJN. "Stability of Ductile Structural Walls." ACI Structural Journal 1993; 77(4): 385-392.
10. Pilakoutas K, Elnashai AS. "Cyclic Behaviour of R.C. Cantilever Walls, Part I: Experimental Results." ACI Structural Journal 1995; 92(3): 271-281.
11. Tasnimi AA. Strength and Deformation of Mid-Rise Shear Walls under Load Reversal. Engineering Structures 2000. 22: 311-322.
12. Moehle JP. "State of Research on Seismic Retrofit of Concrete Building Structures in the US." US-Japan Symposium and Workshop on Seismic Retrofit of Concrete Structures - State of Research and Practice, September 2000
13. FEMA, NEHRP Guidelines for the Seismic Rehabilitation of Buildings, Federal Emergency Management Agency, FEMA 273 (and commentary FEMA 274), October 1997.
14. EUROCODE 2, "Design of Concrete Structures – Part 1-1: General rules and rules for buildings" , ENV 1992-1-1, 1991.